Spontaneous density grating formation in suspensions of dielectric nanoparticles

S. M. WIGGINS, G. R. M. ROBB, B. W. J. MCNEIL, D. R. JONES, S. P. JAMISON and D. A. JAROSZYNSKI
University of Strathclyde, Department of Physics and Applied Physics, Glasgow G4 0NG, UK

(*Received 24 September* 2001)

Abstract. Experimental evidence for nonlinear optical behaviour due to the spontaneous formation of wavelength-scale density modulations or gratings in suspensions of dielectric particles is presented. A collection of dielectric particles pumped by a coherent radiation field may simultaneously form a density grating on the scale of the radiation wavelength and a coherently backscattered radiation field. The particle density grating is generated as a result of a periodic ponderomotive potential formed by the interference of the pump and backscattered fields. The experiment used a water suspension of latex microspheres (radius $\approx$ 56 nm) pumped by a green CW laser (532 nm, power $\leqslant$ 5W). A theoretical model of collective scattering of light from dielectric particles has been extended to include the effects of viscous and Brownian forces on the particles. This model predicts a small degree of particle bunching from which coherent backscattering of the pump occurs. The results of the theoretical model compare favourably with the experimental evidence. The relation between the results presented here and the phenomenon of Collective Rayleigh Scattering (CRS) is discussed.

1. Introduction

Dielectric particles that are small compared with the wavelength of an incident radiation field exhibit Rayleigh scattering behaviour [1]. A new classical scattering phenomenon called 'Collective Rayleigh Scattering' (CRS) has been predicted [2], which involves the spontaneous formation of a particle density modulation on the scale of the radiation wavelength, thereby forming a refractive density grating. Radiation backscattering from such an ensemble of particles is therefore coherent. In the field of nonlinear optics, these density gratings represent potentially novel nonlinear optical media with applications as artificial Kerr media [3], tunable photonic bandgap materials [4] and also to facilitate feedback in random lasers [5].

The grating may be spontaneously generated via the interaction of the particles with a radiation pump field and a small counterpropagating radiation probe field (which may arise from noise due to random fluctuations in the particle density) that produces periodic ponderomotive forces in the particle ensemble. The collective nature of CRS may result in an exponentially growing counterpropagating radiation probe field. The phenomenon is analogous to the periodic bunching of free electrons in the free-electron laser (FEL) [6], and atoms in the collective

Journal of Modern Optics ISSN 0950–0340 print/ISSN 1362–3044 online © 2002 Taylor & Francis Ltd
http://www.tandf.co.uk/journals
DOI: 10.1080/09500340110109025

atomic recoil laser (CARL) [7], both processes resulting in the emission of coherent radiation.

The first results from an experiment designed to observe this phenomenon and the theoretical framework of CRS in a viscous background medium are presented.

The experiment consists of a suspension of latex nanoparticles in water pumped by a green CW laser. A fraction of the backscattered field is coupled into an optical cavity containing the nanoparticle suspension. The use of the cavity should assist in the probe field/nanoparticle coupling and the subsequent formation of a strong particle density grating. Although problems were encountered in optimizing this cavity enhanced coupling, evidence of a weak grating formation was obtained that concurs with theoretical predictions.

2. Experimental set-up

The experimental set-up with the linear cavity is displayed in figure 1. These experiments have been conducted at the University of Strathclyde TOPS user facility [8]. The pump laser is a CW Nd:YVO_4 laser operating at wavelength $\lambda_0 = 532\,\text{nm}$ and power $P \leqslant 5\,\text{W}$. It is focused to a waist $w_0 = 75\,\mu\text{m}$ inside a cubic cuvette of volume $1\,\text{cm}^3$ containing the dielectric particles suspended in water (refractive index $n = 1.33$ and viscosity $\eta = 1.1 \times 10^{-3}\,\text{Nsm}^{-2}$). The particles are latex microspheres of mean radius $a = 56\,\text{nm}$, refractive index $n_1 = 1.59$, density $\rho_p = 1.06 \times 10^3\,\text{kg}\,\text{m}^{-3}$ and number density $N_p \leqslant 10^{12}\,\text{cm}^{-3}$. Their terminal velocity in water is less than $1\,\text{nm}\,\text{s}^{-1}$ so gravitational settling of the particles is negligible in the time frame of the experiment. With the expected evolution of a density grating occurring on a millisecond time scale, convection currents in the background medium due to heating by the pump field can also be neglected as such currents take some seconds to be initiated.

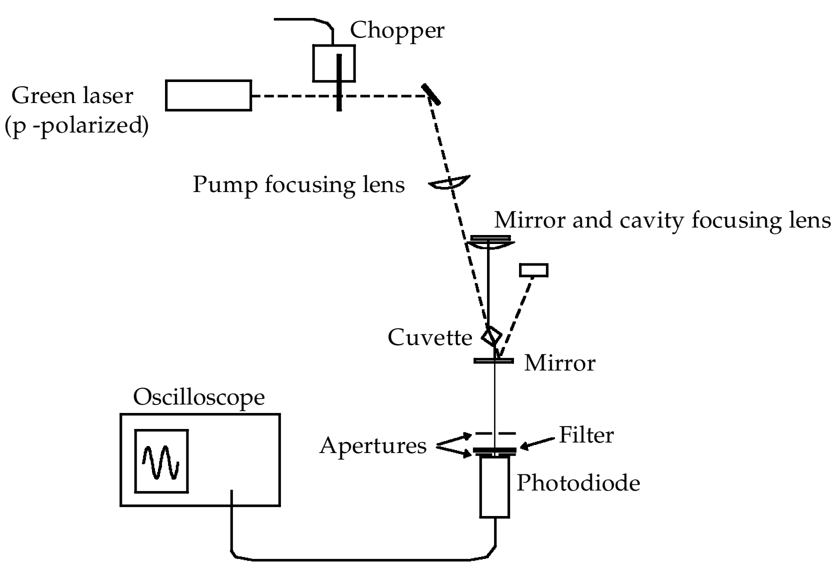

Figure 1. Plan view of experimental set-up.

A fraction of the backscattered radiation from each particle is coupled into a longitudinal mode of a linear cavity. This fraction, determined by the solid angle subtended by the cavity focusing lens, is approximately 10^{-3} of the total scattered field. Owing to a small mis-alignment between the pump and scattered (probe) fields of $\sim 5^\circ$, the pump field is not directly coupled into the cavity mode. This geometry predicts the axis halfway between the pump/cavity axes would form the normal to the planes of any particle density grating. The cavity, of length $L = 21\,\text{cm}$, is formed by two plane dielectric mirrors (coefficient of reflectivity $R = 0.9994$) with a plano-convex lens present to provide stability. The transmitted field at one mirror is detected using a high-bandwidth silicon photodiode with integral amplifier.

Problems were experienced in adjusting the cavity to a resonant mode of the pump frequency, this problem being attributed to the high cavity finesse. In the experiment, therefore, coupling to a cavity mode was small and feedback considerably reduced. The system would then act more as a single-pass amplifier of the small backscattered component of the 'spontaneous radiation' that arises from the random incoherent Rayleigh scattering from the particles. Despite the reduced probe field/nanoparticle coupling, experimental evidence was obtained which demonstrates a nonlinear scattering behaviour of the system consistent with the formation of a density grating of the latex microspheres as predicted by the theoretical model presented in the following section.

The dependence of the probe power in the cavity as a function of the pump power is presented in figure 2 for four different latex particle number densities. Figures 2(a) and (b) are for dilute solutions and figures 2(c) and (d) are for denser solutions. It should be emphasized that for the larger densities the single scattering regime is valid so that the nonlinear behaviour may not be attributed to the effects of multiple scattering. The linear dependence of the probe power is as expected for the dilute solutions. However, for the larger particle densities, a nonlinear dependence of probe power is observed for higher values of the pump power. This nonlinear behaviour is attributed to a small degree of particle bunching.

Modelling

3.1. *Model of Collective Rayleigh Scattering in a viscous medium*

A simple one-dimensional model is used to describe the experiment discussed in the previous section. It consists of a strong plane pump wave, scattered by an initially uniform spatial distribution of dielectric Rayleigh particles suspended in a viscous medium, and an initially very weak counterpropagating plane wave probe, as shown schematically in figure 3.

The form of the $\boldsymbol{E}$-field in the medium is

$$\boldsymbol{E} = \boldsymbol{E}_1(z,t) + \boldsymbol{E}_2(z,t), \tag{1}$$

where $\boldsymbol{E}_1(z,t) = [A_1(z,t)\exp(\mathrm{i}(kz - wt)) + \text{c.c.}]\hat{\boldsymbol{x}}$ is the $\boldsymbol{E}$-field of the initially weak probe field and $\boldsymbol{E}_2(z,t) = [A_2 \exp(-\mathrm{i}(kz + wt)) + \text{c.c.}]\hat{\boldsymbol{x}}$ is the $\boldsymbol{E}$-field of the strong pump field, which we assume here to be of constant amplitude, c/n is the speed of light in the medium, $k = 2\pi/\lambda_m$ is the wavenumber, $\lambda_m = \lambda_0 n$ is the wavelength of the light in the medium, n is the refractive index of the medium and $\hat{\boldsymbol{x}}$ is a transverse unit vector.

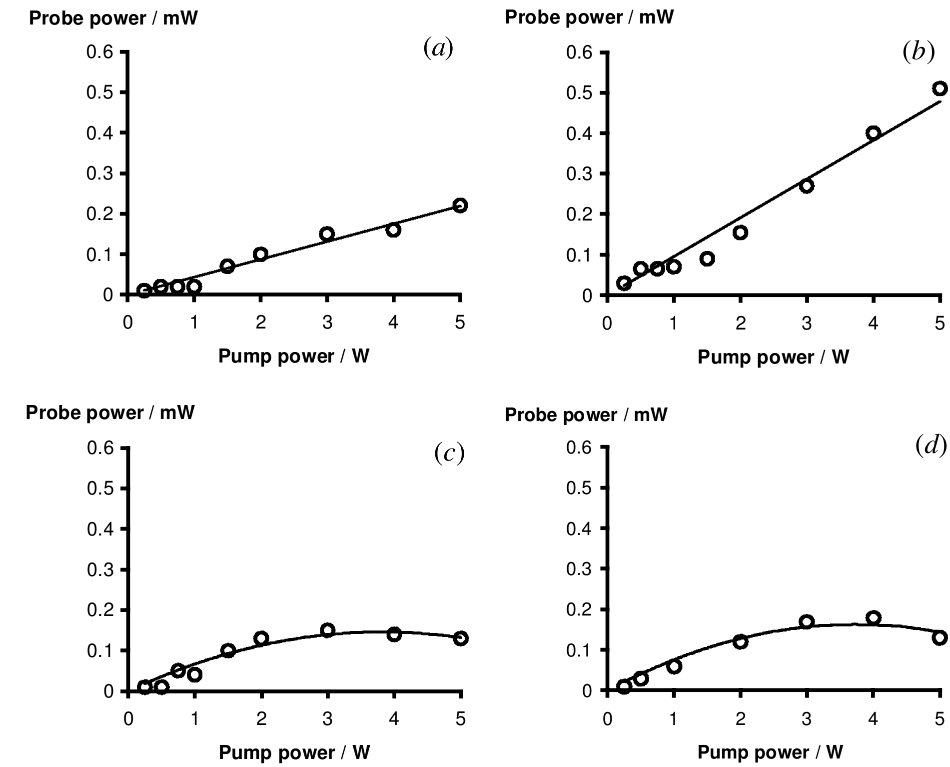

Figure 2. Probe power in the cavity as a function of the pump power for particle number density of (*a*) $9 \times 10^{9}\,\mathrm{cm}^{-3}$, (*b*) $3 \times 10^{10}\,\mathrm{cm}^{-3}$, (*c*) $5 \times 10^{10}\,\mathrm{cm}^{-3}$ and (*d*) $7 \times 10^{10}\,\mathrm{cm}^{-3}$. The curves represent best fit curves.

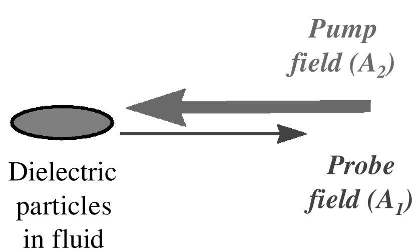

Figure 3. Schematic of CRS experiment.

The force on the jth particle exerted by the optical fields can be derived from the Lorentz force equation to be [2]

$$\boldsymbol{F}_j = \frac{\partial \boldsymbol{d}_j}{\partial t} \times \boldsymbol{B}(z_j, t), \tag{2}$$

where $\boldsymbol{B}(z, t) = (n/c)\hat{\boldsymbol{z}} \times (\boldsymbol{E}_1 - \boldsymbol{E}_2)$ is the magnetic field of the electromagnetic wave, $\boldsymbol{d}_j$ is the dipole moment of the jth particle induced by the $\boldsymbol{E}$-field at $z = z_j$ (the axial position of the jth particle) given by

$$\boldsymbol{d}_j = \varepsilon_0 \varepsilon_m V_p[\chi(A_1(t) \exp(\mathrm{i}(kz - \omega t)) + A_2 \exp(-\mathrm{i}(kz + \omega t))) + \mathrm{c.c.}]\hat{\boldsymbol{x}}. \tag{3}$$

ε_0 is the permittivity of free space, ε_m is the relative permittivity of the viscous medium and $V_p = 4\pi a^3/3$ is the particle volume. The susceptibility of the dielectric particle is $\chi = \chi_1 + i\chi_2$, where

$$\chi_1 = 3\varepsilon_0 \left(\frac{\varepsilon_p - \varepsilon_m}{\varepsilon_p + 2\varepsilon_m} \right)$$

represents the dispersive response of the dipole and

$$\chi_2 = 2(ka)^3 \varepsilon_0^2 \left(\frac{\varepsilon_p - \varepsilon_m}{\varepsilon_p + 2\varepsilon_m} \right)^2$$

represents the dissipative response of the dipole, due to damping via re-radiation, i.e. incoherent Rayleigh scattering. Substituting for $\boldsymbol{B}$ and $\boldsymbol{d}_j$ in equation (2) and following the derivation described in [2], the dynamics of the particles under the influence of the electromagnetic fields, the viscous drag force due to the medium and the stochastic Brownian forces exerted on the particle by the molecules of the suspending medium are described by

$$\frac{dz_j}{dt} = \frac{p_j}{M}, \tag{4}$$

$$\frac{dp_j}{dt} = 2\varepsilon_0 V_p [i\chi A_2 (A_1(t) \exp(2ikz_j) - \text{c.c.}) + \chi_2 (|A_1(z,t)|^2 - A_2^2)] - \gamma p_j + f(t), \tag{5}$$

where p_j is the z-component of the momentum of the jth particle, $\gamma = 6\pi a\eta/M$ is the viscous momentum damping coefficient derived from Stokes law, $f(t)$ is a randomly fluctuating force and M is the mass of the particle.

The dynamics of the probe field are found from Maxwell's wave equation:

$$\left(\frac{\partial^2}{\partial z^2} - \frac{n^2}{c^2} \frac{\partial^2}{\partial t^2} \right) \boldsymbol{E}(z,t) = \mu_0 \frac{\partial^2 \boldsymbol{P}(z,t)}{\partial t^2} \tag{6}$$

where μ_0 is the permeability of free space and $\boldsymbol{P}(z,t)$ is a macroscopic polarization arising from the contributions of the dipole moments of all the particles, i.e.

$$\boldsymbol{P}(z,t) = \sum_{j=1}^{N} \boldsymbol{d}_j \delta(\boldsymbol{r} - \boldsymbol{r}_j(t)). \tag{7}$$

Substituting for $\boldsymbol{E}$ and $\boldsymbol{d}_j$ and again following the derivation of [2], it can be shown that the evolution of the complex amplitude of the probe field, $A_1(t)$, is described by

$$\frac{\partial A_1}{\partial z} + \frac{n}{c}\frac{\partial A_1}{\partial t} = \frac{ikV_p \chi N_p}{2} (A_2 \langle \exp(i\theta) \rangle + A_1) \tag{8}$$

where

$$\langle \ldots \rangle = \frac{1}{N} \sum_{j=1}^{N} (\ldots)_j$$

denotes a local average over the ensemble of N particles in a ponderomotive potential.

Equations (4), (5) and (8) can be reduced to a universally scaled form using the dimensionless parameters

$$\theta_j = 2kz_j, \quad \bar{p}_j = \frac{p_j}{\rho M c^2}, \quad \bar{t} = 2\omega\rho t, \quad \bar{z} = 2k\rho z,$$
$$\bar{A}_1 = -2i\sqrt{\frac{\varepsilon_0\varepsilon_m}{\rho N_p M c^2}}A_1, \quad \bar{\gamma} = \frac{3\pi a\eta}{\omega\rho M}, \quad \alpha = \frac{\chi_2}{\chi_1}, \quad \rho = \frac{N_p V_p \chi_1}{4}, \tag{9}$$

where $\bar{\gamma}$, α and ρ are dimensionless viscous damping, incoherent scattering and coupling parameters, respectively. Using these parameters, the evolution of the particles and fields are described by:

$$\frac{\partial\theta_j}{\partial\bar{t}} = \bar{p}_j, \tag{10a}$$

$$\frac{\partial\bar{p}_j}{\partial\bar{t}} = -(\bar{A}_1\bar{A}_2^* \exp(\mathrm{i}\theta) + \text{c.c.}) + \alpha(|\bar{A}_1|^2 - \bar{A}_2^2) - \bar{\gamma}\bar{p}_j + f(t), \tag{10b}$$

$$\frac{\partial\bar{A}_1}{\partial\bar{t}} + \frac{\partial\bar{A}_1}{\partial\bar{z}} = (1 + \mathrm{i}\alpha)(\bar{A}_2\langle\exp(\mathrm{i}\theta)\rangle + \mathrm{i}\bar{A}_1). \tag{10c}$$

The initial conditions for equations (9) correspond to a very weak probe field intensity and particles with a uniform distribution of positions and a Gaussian momentum distribution with width σ_p given by

$$\sigma_p = \frac{n}{\rho}\sqrt{\frac{k_B T}{Mc^2}}$$

where k_B is Boltzmann's constant and T is the temperature.

In the limit of strong viscous damping, it is possible to eliminate adiabatically the particle momentum variables $\bar{p}_j$, so that equations (10a) and (10b) reduce to

$$\frac{\partial\theta_j}{\partial\bar{t}} = -\frac{1}{\bar{\gamma}}(\bar{A}_1\bar{A}_2^* \exp(\mathrm{i}\theta_j) + \text{c.c.}) + \frac{\alpha}{\bar{\gamma}}(|\bar{A}_1|^2 - \bar{A}_2^2) + \frac{f(t)}{\bar{\gamma}}. \tag{11}$$

This equation, which describes the evolution of the particle positions (θ_j) under the action of a position-dependant deterministic force and a stochastic force, can be replaced by a Fokker–Planck equation describing the evolution of the particle probability distribution $P(\theta, \bar{t})$.

$$\frac{\partial P(\theta,\bar{t})}{\partial\bar{t}} = -\frac{\partial}{\partial\theta}\left[\left(-\frac{1}{\bar{\gamma}}(\bar{A}_1\bar{A}_2^* \exp(\mathrm{i}\theta) + \text{c.c.}) + \frac{\alpha}{\bar{\gamma}}(|\bar{A}_1|^2 - \bar{A}_2^2)\right)P(\theta,\bar{t})\right]$$
$$+ \bar{\gamma}\sigma^2\frac{\partial^2 P(\theta,\bar{t})}{\partial\theta^2}. \tag{12a}$$

Similarly, the probe field evolution equation (10b) can be replaced by

$$\frac{\partial\bar{A}_1}{\partial\bar{t}} + \frac{\partial\bar{A}_1}{\partial\bar{z}} = (1 + \mathrm{i}\alpha)\left(\bar{A}_2\int P(\theta,\bar{t})\exp(\mathrm{i}\theta)\,\mathrm{d}\theta + \mathrm{i}\bar{A}_1\right). \tag{12b}$$

Assuming $P(\theta, \bar{t})$ is periodic in θ, equations (12a,b) can be written in terms of the spatial harmonics of $P(\theta, \bar{t})$, i.e. $P(\theta, \bar{t}) = \sum_k P_k(\bar{t})\exp(\mathrm{i}k\theta)$

$$\frac{\mathrm{d}P_k}{\mathrm{d}t} = \mathrm{i}\frac{k}{\bar{\gamma}}(\bar{A}_1\bar{A}_2^* P_{k-1} + \bar{A}_1^*\bar{A}_2 P_{k+1}) - k\left(\frac{\mathrm{i}}{\bar{\gamma}}\alpha(|\bar{A}_1|^2 - |\bar{A}_2|^2) + \bar{\gamma}\sigma_p^2 k\right)P_k, \tag{13a}$$

where $P_0 = 1/2\pi$ and $P_{-n} = P_n^*$. Consequently, the probe evolution equation (12b) becomes

$$\frac{\partial \bar{A}_1}{\partial \bar{t}} + \frac{\partial \bar{A}_1}{\partial \bar{z}} = (1 + \mathrm{i}\alpha)(2\pi \bar{A}_2 P_1 + \mathrm{i}\bar{A}_1). \qquad (13b)$$

It can be seen from equation (13*b*) that a particle density modulation (P_1) can couple the pump and probe fields. The nature of the coupling depends on the strength and the phase of the density modulation, i.e. the position in the ponderomotive potential around which the particles bunch.

3.2. *Explanation of experimental results from a CRS-like model*

Equations (13*a*,*b*) are solved under steady-state conditions ($\partial/\partial\bar{t} = 0$) neglecting spatial harmonics of $P(\theta, \bar{t})$ higher than the first. Assuming $|\bar{A}_1| \ll |\bar{A}_2|$, and $|\bar{A}_2|^2 \ll \bar{\gamma}\sigma_p^2/\alpha$, as is the case for the experiments described earlier, the steady-state solution for P_1 is:

$$P_1 = \mathrm{i}\frac{\bar{A}_1\bar{A}_2^*}{2\pi\bar{\gamma}^2\sigma_p^2}, \qquad (14a)$$

so that the steady-state equation for the probe field is

$$\frac{\mathrm{d}\bar{A}_1}{\mathrm{d}\bar{z}} = (1 + \mathrm{i}\alpha)(2\pi\bar{A}_2 P_1 + \mathrm{i}\bar{A}_1), \qquad (14b)$$

which can be combined to give a single equation for the probe intensity $\bar{I}_1 = \bar{A}_1\bar{A}_1^*$.

$$\frac{\mathrm{d}\bar{I}_1}{\mathrm{d}\bar{z}} = -2\alpha\left(1 + \frac{\bar{I}_2}{\bar{\gamma}^2\sigma_p^2}\right)\bar{I}_1 + \bar{I}_s, \qquad (15)$$

where $\bar{I}_2 = \bar{A}_2\bar{A}_2^*$ is the scaled pump intensity and $\bar{I}_s$ is a phenomenological seed or source field, defined as

$$\bar{I}_s = f\left(-\frac{\mathrm{d}\bar{I}_2}{\mathrm{d}\bar{z}}\right) = 2\alpha f \bar{I}_2.$$

Physically, this incoherent seed field arises from the fraction, f, of the pump field intensity which is Rayleigh scattered into the solid angle subtended by the cavity focusing lens. The solution of (14) is

$$\bar{I}_1(\bar{z}) = \frac{f\bar{I}_2}{\left(\frac{\bar{I}_2}{\bar{\gamma}^2\sigma_p^2} + 1\right)}\left[1 - \exp\left(-2\alpha\right)\left(\frac{\bar{I}_2}{\bar{\gamma}^2\sigma_p^2} + 1\right)\bar{z}\right] \qquad (16)$$

It can be seen from (16) that for $\bar{I}_2 \ll \bar{\gamma}^2\sigma_p^2$, the probe field intensity depends linearly on the pump intensity, i.e. $\bar{I}_1 \propto \bar{I}_2$. By contrast, for scaled pump intensities $\bar{I}_2 \approx \bar{\gamma}^2\sigma_p^2$ or greater, the probe field intensity has a nonlinear dependence on the pump intensity. Using parameters that correspond to the graphs shown in figure 2, i.e. $a = 56\,\mathrm{nm}$, $\lambda_0 = 532\,\mathrm{nm}$, $\varepsilon_m = n^2 = 1.77$, $\varepsilon_p = 2.56$, sample length $L = 1.3\,\mathrm{cm}$, $\eta = 1.1 \times 10^{-3}\,\mathrm{Nsm^{-2}}$, $\mathrm{w_o} = 75\,\mu\mathrm{m}$, $T = 300\,\mathrm{K}$ and $f = 1 \times 10^{-3}$, equation (16) predicts the variation of probe power as a function of pump power for different particle number densities as shown in figure 4.

From a comparison of figures 3 and 4, it can be seen that equation (16) describes the transition of the dependence of the probe power on the pump power from approximately linear for the most dilute samples to strongly nonlinear for the densest samples.

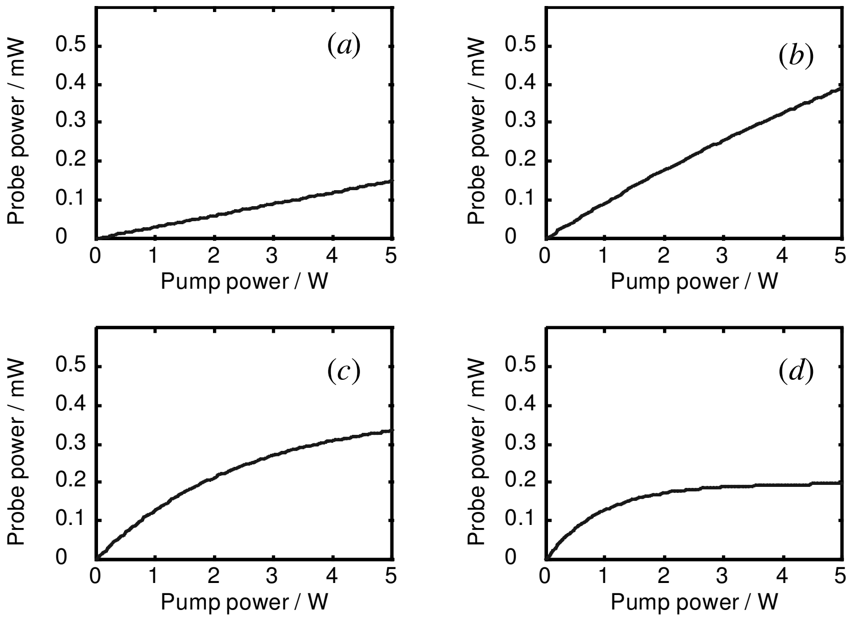

Figure 4. Probe power as a function of the pump power as calculated from equation (16) for particle number density (*a*) $9 \times 10^9\,\mathrm{cm}^{-3}$, (*b*) $3 \times 10^{10}\,\mathrm{cm}^{-3}$, (*c*) $5 \times 10^{10}\,\mathrm{cm}^{-3}$ and (*d*) $7 \times 10^{10}\,\mathrm{cm}^{-3}$.

The origin of this nonlinearity is a spatial modulation in the particle number density (P_1) with period $\approx\lambda/2$. It can be seen from equation (14) that the effect of the density modulation is to increase the rate of loss of the probe field due to incoherent Rayleigh scattering by a factor

$$1 + \frac{\bar{I}_2}{\bar{\gamma}^2 \sigma_p^2}.$$

This factor arises from the fact that the dipole moment on each particle is induced by *both* the pump and probe fields. The evolution of the probe field is determined by the component of the polarization wave produced by the collection of oscillating dipoles which copropagates with the probe field, i.e. the RHS of equation (8) or equation (14). Let us consider three cases:

(i) In the absence of the pump field ($\bar{A}_2 = 0$), the polarization wave is simply proportional to the probe field ($\bar{A}_1$) and attenuation of the probe due to ordinary incoherent Rayleigh scattering occurs.

(ii) In the presence of the pump field ($\bar{A}_2 \neq 0$) but when the particles are fixed and uniformly distributed in space ($\langle \exp(-\mathrm{i}\theta) \rangle = P_1 = 0$), the component of the polarization wave copropagating with the probe field is still simply proportional to the probe field, as the contribution from the pump field to the dipole moment of each particle averages to zero.

(iii) In the presence of the pump field ($\bar{A}_2 \neq 0$) but when the particle density distribution is spatially periodic ($\langle \exp(-\mathrm{i}\theta) \rangle, P_1 \neq 0$), the component of the polarization wave copropagating with the probe field is greater than that arising from the probe field alone. The additional contribution to the dipole moment of each particle, which arises from the pump field, adds up coherently owing to the spatial modulation in the particle density distribution. This increased dipole amplitude leads to an increased rate of re-radiation (incoherent Rayleigh scattering) and attenuation of the probe field. This is the physical reason for the saturation of the probe power for high densities, where the additional coherent contribution to the polarization amplitude is strongest.

It is useful at this point to discuss the relationship between the results presented here and the phenomenon of CRS first predicted in [2]. In the original theoretical studies of CRS, the particles were not assumed to be suspended in a viscous medium but were assumed to be free in vacuum, and incoherent Rayleigh scattering was neglected ($\alpha = 0$). It was shown in [2] that a backscattered probe field and a particle density modulation could be strongly amplified in such a system owing to strong particle bunching in a periodic ponderomotive potential. The inclusion of viscous effects, incoherent Rayleigh scattering ($\alpha > 0$) and Brownian particle motion in the CRS model opens the possibility of other types of behaviour in addition to the original CRS. The results presented here show that the backscattered field and density modulation produced in our experiments are weak, although sufficient to produce nonlinear optical behaviour. In true CRS, as originally described in [2], the probe field can be amplified to values comparable to that of the pump and very strong density modulations can be produced.

An important distinction between true CRS and the phenomena described here is the position in the ponderomotive potential about which the particles bunch, relative to the light intensity distribution. In true CRS, the particle density modulation and the standing-wave intensity modulation formed by the counter-propagating fields are approximately in phase and a dynamic phase shift of the probe field, similar to that which occurs in the high-gain FEL [6] allows a large energy exchange from pump to probe. By contrast, for the system described here where viscous effects play a major role, it can be seen from equation (14a) that the particle density modulation (P_1) and the intensity modulation are $\pi/2$ out of phase ($P_1 \propto i\bar{A}_1\bar{A}_2^*$). In addition, as equation (16) contains no phase information, the phase of the probe field does not play a signficant role in the interaction. These conditions prohibit significant energy exchange from pump to probe. Consequently, while the phenomena described in this paper contain many features in common with CRS, namely nonlinear optical behaviour of a backscattered field resulting from the spontaneous generation of a particle density modulation, they also exhibit significant differences from true CRS as originally described in [2], e.g. the induced modulation does not behave as a reflective grating but as a dissipative grating structure.

4. Conclusion

Experimental evidence for nonlinear optical behaviour due to the spontaneous formation of wavelength-scale density modulations or gratings in suspensions of dielectric particles has been presented. The particle density grating is generated as a result of a periodic ponderomotive potential formed by the interference of the pump and backscattered (probe) fields. It has been shown that the experimental results are well described using a model originally developed to investigate CRS.

The results of the experiment and theory indicate that the system is currently operating in a regime where the backscattered fields and the spontaneous density gratings are of small amplitude, although sufficiently large to produce nonlinear optical behaviour. After refining aspects of this experiment, e.g. increasing the cavity Q-factor, and using further predictions from the CRS model based on the agreement observed to date, the prospects for future observation of the true CRS regime with spontaneous high-gain amplification of the backscattered field as originally predicted in [2] are encouraging.

Acknowledgments

We thank the EPSRC and Royal Society of Edinburgh for supporting this work.

References

[1] Miles, R. B., Lempert, W. R., and Forkey, J. N., 2001, *Meas. Sci. Technol.,* **12,** R33.
[2] McNeil, B. W. J., and Robb, G. R. M., 1998, *Opt. Commun.,* **148,** 54.
[3] Smith, P. W., Maloney, P. J., and Ashkin, A., 1982, *Opt. Lett.,* **7,** 347.
[4] Moroz, A., 2000, *Europhys. Lett.,* **50,** 466.
[5] Cao, H., Zhao, Y. G., Ho, S. T., Seelig, E. W., Wang, Q. H., and Chang, R. P. H., 1999, *Phys. Rev. Lett.,* **82,** 2278.
[6] Bonifacio, R., Casagrande, F., Cerchioni, G., De Salvo Souza, L., Pierini, P., and Piovella, N., 1990, *Rivista del Nuovo Cimento,* **13,** 9.
[7] Bonifacio, R., De Salvo, L., Narducci, L. M., and D'angelo, E. J., 1994, *Phys. Rev.* A, **50,** 1716.
[8] Jaroszynski, D. A., Ersfeld, B., Giraud, G., Jamison, S. P., Jones, D. R., Issac, R. C., McNeil, B. W. J., Phelps, A. D. R., Robb, G. R. M., Sandison, H., Vieux, G., Wiggins, S. M., and Wynne, K., 2000, *Nucl. Instrum. Methods Phys. Res., Sect. A,* **445,** 317.